Analytical Biochemistry, Full-length Article

Title:

Kinetic analyses of two-steps oxidation from L-tyrosine to L-dopaquinone with tyrosinase by capillary electrophoresis/dynamic frontal analysis

Author names and affiliations:

Masanori Mine,[1] Hitoshi Mizuguchi,[2] Toshio Takayanagi[2,*]

1 *Graduate School of Advanced Technology and Science, Tokushima University, 2-1 Minamijyousanjima-cho, Tokushima 770-8506, Japan*

2 *Graduate School of Technology, Industrial and Social Sciences, Tokushima University, 2-1 Minamijyousanjima-cho, Tokushima 770-8506, Japan*

Corresponding author:

E-mail addresses: toshio.takayanagi@tokushima-u.ac.jp (T. T.)

TEL & FAX: +81-88-656-7409

Abstract

Tyrosinase catalyzes the oxidation of L-tyrosine in two stages to produce L-dopa and L-dopaquinone stepwise, and L-dopaquinone is subsequently converted to dopachrome. Most of the conventional analyses subjected only one-step reaction from L-tyrosine to L-dopa or from L-dopa to L-dopaquinone. In this study, kinetic analyses of two-steps oxidation of L-tyrosine with tyrosinase were made by capillary electrophoresis/dynamic frontal analysis (CE/DFA). When L-dopa was introduced into a capillary as a sample plug in a CE/DFA format, the enzymatic oxidation continuously occurred during the electrophoresis, and the product L-dopaquinone was subsequently converted to dopachrome which was detected as a plateau signal. A Michaelis-Menten constant of the second-step kinetic reaction, $K_{m,Do}$, was determined as 0.45±0.03 mmol L^{-1}. In the analysis of the first-step kinetic reaction from L-tyrosine to L-dopa, L-dopa was not resolved by CE/DFA because both L-tyrosine and L-dopa are electrically neutral. The L-dopa formed and co-migrated at the L-tyrosine zone was calibrated beforehand with the final product of dopachrome detected as a plateau signal. Constantly formed L-dopa was successfully detected as a plateau signal of dopachrome, and a Michaelis-Menten constant of $K_{m,Ty}$ was also determined as 0.061±0.009 mmol L^{-1} by the CE/DFA. CE/DFA is applicable to two-steps enzymatic reactions.

Keywords

Capillary electrophoresis, Dynamic frontal analysis, Tyrosinase, Two-steps oxidation, Kinetic analysis

Declaration of interest:

Funding: This work was supported by a Grant-in-Aid for Scientific Research (C) (No. 20K05568) from the Japan Society for the Promotion of Sciences (JSPS).

Competing interests: The authors declare that they have no conflict of interest.

Authors' contributions: **M. M.**: Methodology, Investigation, Data curation, Formal analysis, Visualization, Writing - original draft; **H. M.**: Resources, Validation; **T. T.**: Conceptualization, Funding acquisition, Project administration, Supervision, Writing - review & editing.

1. Introduction

Tyrosinase (TRS; EC1.14.18.1) is an enzyme that catalyzes the *o*-hydroxylation of monophenols, as well as the oxidation of *o*-diphenols to *o*-quinones. It is widely present in microorganisms, animal and plant tissues [1]. A final product of melanin is generated with TRS from L-tyrosine *via* L-3,4-dihydroxyphenylalanine (L-dopa) and dopaquinone [2]. Melanin is an essential pigment on browning of fruits and vegetables, as well as the development of insects in living organisms [3,4]. For mammals, the degree and distribution of melanin pigmentation is the most important factor in skin and hair color, and the role of melanin is to protect the skin from UV damage by absorbing UV and removing reactive oxygen species. On the other hand, enzymatic browning with melanin is recognized as one of major problems in food industry for fruit, vegetable, and seafood products [5]. Excessive levels of epidermal pigmentation accumulate due to various skin disorders [6]. Therefore, TRS is an important enzyme in melanin biosynthesis.

Figure 1 shows a reaction diagram of tyrosine oxidation with TRS [7]. TRS catalyzes the reactions from L-tyrosine (Ty) to L-dopa (Do) and from Do to dopaquinone (Dq). The product Dq is an unstable intermediate, and it is instantly converted to dopachrome (Dc) [7]. Dopachrome is generally detected as a reaction product from Do with TRS [8,9]. Dopachrome is further converted, and melanin is finally generated [7].

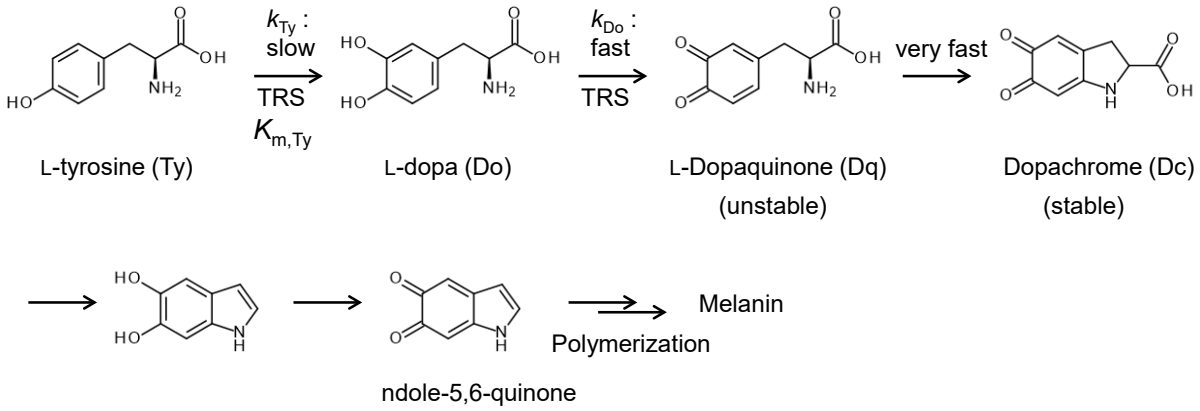

Fig. 1. Reaction diagram of tyrosine oxidation with tyrosinase (TRS). Formed L-dopaquinone is further converted to dopachrome, 5,6-dihydroxyindole, and indole-5,6-quinone. Melanin is finally generated.

Capillary electrophoresis (CE) is one of major analysis methods for enzymatic reactions based on its high resolution and small consumption volume [10]. CE-based enzymatic analyses are broadly classified into pre-capillary and in-capillary reactions [11]. The in-capillary format includes electrophoretically mediated

microanalysis (EMMA) [12-14], pressure-mediated microanalysis (PMMA) [15], enzyme-immobilized microreactor (IMER) [16-18], and laminar flow profile transverse diffusion (TDLFP) [19,20]. As for the tyrosinase activity, studies have been reported by pre-capillary reactions [7], IMER [21,22], EMMA [23], PMMA [24], and chiral ligand exchange capillary electrophoresis [25,26]. The reported studies, however, simply performed traditional batch reactions in a capillary, because the reaction proceeded without electrophoretic migration. Therefore, the reactions would not be in a steady state, and any product inhibition would be unavoidable, even if the reaction time is set as shortest to suppress the product inhibition.

On the other hand, in capillary electrophoresis/dynamic frontal analysis (CE/DFA) [27], the reaction product is immediately and continuously resolved from the substrate zone during the electrophoresis. CE/DFA possesses such a characteristic that the enzymatic reaction proceeds at a steady state without product inhibition. Plateau signals are generally detected in CE/DFA based on a zero-order enzymatic reaction, and the height of the plateau signal directly reflects the reaction rate. Enzymatic reactions can be analyzed through the height of the plateau signal without any inhibition by the product. The flat plateau signal also suggests that the enzymatic reaction is in a steady state and a practical Michaelis-Menten analysis is applicable. CE/DFA was applied to the inhibition analyses with alkaline phosphatase [28] and carboxylesterase [29]. A competition toward substrates was also analyzed with galactosidase [30]. Reversible reactions of transphosphorylation with creatine kinase were also analyzed by a CE/DFA without product inhibitions [31]. To obtain a plateau signal in CE/DFA, two issues are essential about the reaction rate of the enzymatic reaction and the electrophoretic resolution. When the reaction rate is too fast, the substrate is quickly consumed and any plateau signal is not detected. On the other hand, sufficient height of the plateau signal can not be detected, if the reaction rate is too slow. Concerning the second issue, a plateau signal is detected based on the continuous electrophoretic resolution of the product from the substrate zone. Therefore, plateau signal will not be detected when the electrophoretic mobility between a substrate and a product is close with each other.

In this study, CE/DFA was examined to the two steps oxidation of L-tyrosine with TRS, as shown in Fig. 1. The two-steps oxidation reactions were independently analyzed by using Ty or Do as a substrate, and Dc as a detection species. Michaelis-Menten constants of the stepwise reactions ($K_{m,Ty}$ and $K_{m,Do}$) were also determined by the CE/DFA. While all CE studies on TRS activity reported were of batch reactions, and the analyses were limited with one of the stepwise reactions such as from Ty to Do [21] or from Do to Dc [22-24], the two-steps reactions have successfully been analyzed by the proposed CE/DFA. Both K_m values obtained

by the CE/DFA were in good agreement with the literature values, as well as the pre-capillary evaluations in this study. It has been suggested that CE/DFA avoids the product inhibition and accurate K_m values would be determined in stepwise enzyme reactions.

2. Schematic diagram on the analyses from L-tyrosine to L-dopa and from L-dopa to dopaquinone in CE/DFA

Figure 2 shows schematic diagrams of tyrosine oxidations in a capillary by CE/DFA. The oxidations include: (A) from Ty to Do, and (B) from Do to Dq. When Do is used as a substrate in CE/DFA (Fig. 2B), the story is simple as reported in our previous CE/DFA studies [27,29]. Dq is enzymatically produced from Do, and the formed Dq is electrophoretically resolved from the substrate Do zone, because Do is electrically neutral and Dq is anionic at a pH condition of 7.0 suited for the enzymatic reaction. Since the conversion from Dq to Dc is very fast, Dc is a detected species in CE/DFA. When the kinetic reaction from Do to Dq is at a steady state, Dc would be detected as a plateau signal, as illustrated in Fig. 2B(d).

On the other hand, two-steps enzymatic reactions should be considered on the first-step oxidation from Ty to Do. When Ty is used as a substrate (Fig. 2A), Do and Dq are stepwisely generated with TRS. A substrate Ty and the product Do are electrically neutral at pH 7.0, and they migrate together with the electroosmotic flow. Do is further oxidized to Dq, and anionic Dq is immediately resolved from the substrate zone by CE; Dc is similarly a detected species in CE/DFA. The oxidation reaction from Ty to Do is very slow compared to the oxidation of Do to Dq [7]. Therefore, the produced Do is rapidly converted to Dq. Although Ty and Do are not resolved electrophoretically, the formation rate of Dq is related with the steadily generated Do from the substrate Ty. When kinetic reactions from Ty to Do and from Do to Dq are at steady states, the formation rate of Dq or Dc is constant and Dc would be detected as a plateau signal, as illustrated in Fig. 2A(d). We can deduce the constantly generated Do through the plateau signal of Dc.

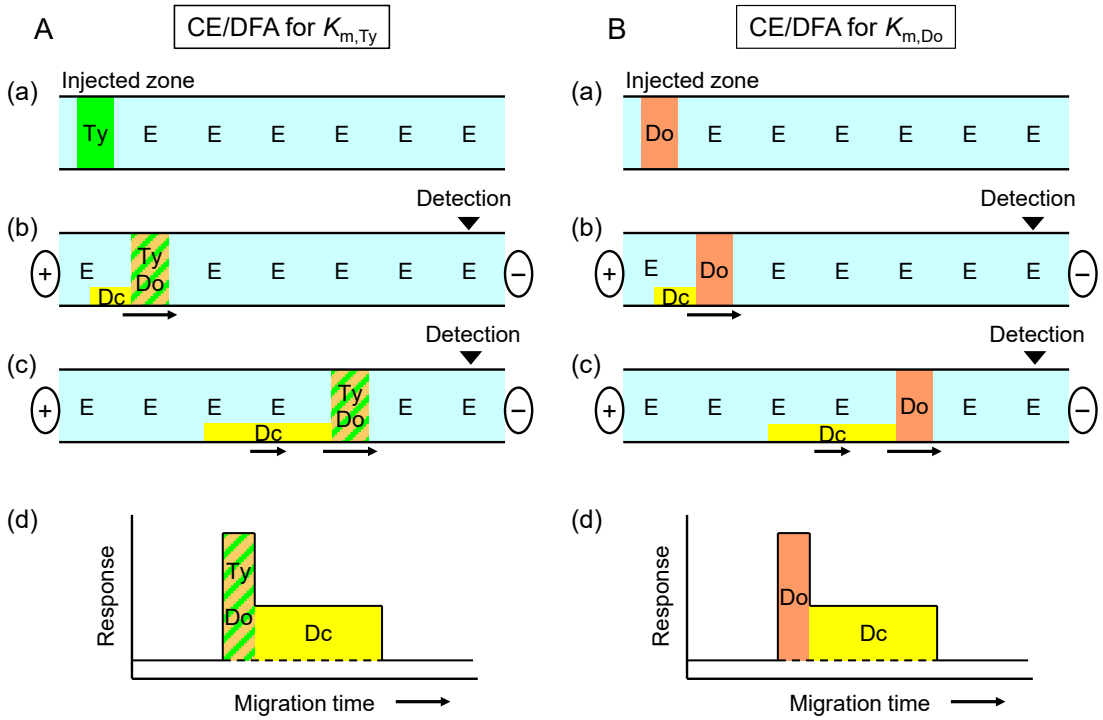

Fig. 2 Schematic migration diagrams on the analyses of tyrosinase oxidation by CE/DFA. An enzyme (E) is contained in the separation buffer. The substrate is: A, Ty and B, Do. (a) - (c) show the electrophoretic migration of the substrate and the product(s) under the enzymatic oxidation(s); final product Dc is continuously generated from the substrate zone, and it electrophoretically migrates toward the anodic end. Continuously generated Dc would be detected as a plateau signal in the illustrated electropherogram (d).

3. Material and methods

3.1 Materials and reagents

Tyrosinase (TRS; from mushroom, EC: 1.14.18.1) was obtained from Sigma-Aldrich (St. Louis, MO, USA). L-Tyrosine and 3-(3,4-dihydroxyphenyl)-L-alanine (L-dopa) were from Tokyo Chemical Industry (Tokyo, Japan). Other reagents were of analytical grade. All solutions were prepared with purified water prepared by Milli-Q Gradient A10 (Millipore, Milford, MA, USA).

3.2 Apparatus

All CE experiments were performed by a ^{3D}CE system (Agilent Technologies, Waldbronn, Germany) quipped with a photodiode array detector. A fused-silica capillary (GL Sciences, Tokyo, Japan) was set in a cassette cartridge, and the cartridge was installed in the CE system. The capillary cartridge was thermostat at

30 °C by circulating constant temperature air. In the CE measurements on pre-capillary reactions, a capillary was used with its total length of 48.5 cm and the effective length from the injection end to the detection point of 40.0 cm. Another capillary was also used in the CE/DFA measurements; its total length was 32.5 cm and the effective length was 24.0 cm. Inner and outer diameters of the capillaries were commonly 75 μm and 375 μm, respectively. The inner wall of the capillary was refreshed daily by flushing with 0.1 mol L^{-1} NaOH for 2 min followed with purified water for 2 min. An Agilent Technologies ChemStation software (Ver. B04.02) was used for the control of the CE system, the data acquisition, and the data analysis.

A Horiba F-71 pH meter was used for controlling the pH of the separation buffers.

3.3 Procedures for the CE and the CE/DFA

3.3.1 Pre-capillary reactions for the determinations of $K_{m,Ty}$ and $K_{m,Do}$

When a kinetic reaction from Ty to Do was examined, solutions containing 0.02−0.2 mmol L^{-1} Ty, 0.02 mg mL^{-1} TRS, and 10 mmol L^{-1} phosphate buffer (pH 7.0) were prepared and they were used as sample solutions for the CE measurements. The reaction was carried out in a vial tray in the CE system controlled at 30 °C. The reaction period was from the addition of TRS to the sample solution to the start of the electrophoresis. The reaction time was set at 5, 10, or 15 min. After the reaction period, the incubated solution was hydrodynamically injected into the separation capillary from the anodic end at 50 mbar for 3 s. After both ends of the capillary were dipped in the separation buffer vials containing 10 mmol L^{-1} borax buffer (pH 9.2), a DC voltage of 25 kV was applied to the capillary. Both products of Do and Dc, as well as the substrate Ty, were photometrically detected at 214 nm. Peak areas of Do and Dc were used for the kinetic analysis. Measurements were made with 3 times to assure the reproducibility.

When a kinetic reaction from Do to Dq was examined, solutions containing 0.1−3.8 mmol L^{-1} Do, 0.004 mg mL^{-1} TRS, and 10 mmol L^{-1} phosphate buffer (pH 7.0) were prepared and they were also used as sample solutions. The reaction temperature and the reaction time were similarly 30 °C and 5, 10, or 15 min. The CE conditions are the same as in the reaction from Ty to Do.

3.3.2 Kinetic analysis from L-dopa to dopaquinone by CE/DFA

Solutions containing 0.1−1.0 mmol L^{-1} Do as a substrate and 10 mmol L^{-1} phosphate buffer (pH 7.0) were prepared, and they were used as sample solutions in CE/DFA measurements. A separation buffer was

prepared with 10 mmol L^{-1} phosphate buffer (pH 7.0) with 0.02 mg mL^{-1} TRS. After the separation capillary being filled with the separation buffer, the substrate solution was hydrodynamically injected into the capillary from the anodic end at 50 mbar for 3 s. Both ends of the capillary were dipped in the separation buffer vials, and a voltage of 20 kV was applied for the CE/DFA. A substrate Do and the product Dc were photometrically detected at 214 nm, and a plateau signal of Dc was obtained. The plateau height of Dc was used for the determination of $K_{m,Do}$.

3.3.3 Kinetic analysis from L-tyrosine to L-dopa by CE/DFA

Both the substrate Ty and the product Do are electrically neutral at the pH condition of 7.0, and they are not resolved by CE. Therefore, quantification of the formed Do is necessary for the kinetic analysis. Since Do is an intermediate species in the enzymatic reaction and it is further converted to Dq and Dc, the formed Do was quantified through the plateau height of Dc. A series of Do solutions were prepared in the concentration range between 0.01−0.05 mmol L^{-1}, and the TRS in the separation buffer was set at 0.08 mg mL^{-1}. A calibration graph for Do was made with the plateau height of Dc in CE/DFA.

Solutions containing 0.02−0.4 mmol L^{-1} Ty as a substrate and 10 mmol L^{-1} phosphate buffer (pH 7.0) were prepared, and they were used as sample solutions in CE/DFA measurements. A separation buffer was prepared with 10 mmol L^{-1} phosphate buffer (pH 7.0) with 0.08 mg mL^{-1} TRS; the concentration of TRS is the same as in the preparation of the calibration graph of Do. After the separation capillary being filled with the separation buffer, the substrate solution was hydrodynamically injected into the capillary from the anodic end at 50 mbar for 3 s. Both ends of the capillary were dipped in the separation buffer vials, and a voltage of 12 kV was applied for the CE/DFA. The substrate Ty, the intermediate Do, and the Dc were detected at 214 nm. A plateau signal was detected with Dc, and it was used for the quantification of steadily generated Do from Ty and for the determination of $K_{m,Do}$.

3.3.4 Determination of Michaelis-Menten constants

Michaelis-Menten constant is popularly determined with Eq. (1).

$$v = \frac{V_{max}[S]}{K_m + [S]} \quad (1)$$

where [S] is the initial concentration of a substrate S, v and V_{max} are the reaction rate and the maximum reaction

rate, and K_m is the Michaelis-Menten constant. In the pre-capillary reaction analysis, two Michaelis-Menten analyses were made with Ty as a substrate for the determination of $K_{m,Ty}$ using the peak areas of the intermediate Do or the final product Dc. Another Michaelis-Menten analysis was also made with Do as a substrate for the determination of $K_{m,Do}$ using the peak area of Dc. The Michaelis-Menten constants were determined with Eq. (1) by a nonlinear least-squares analysis on an R program (Ver 4.0.3) [32]. A series of data set of the substrate concentration [S] and the reaction rate v were input in the analysis, and a value of K_m was optimized.

In the CE/DFA analysis, plateau height of the product Dc was directly used in the Michaelis-Menten analysis, because the plateau height is directly related with the reaction rate [27].

4. Results and Discussion

4.1 Determination of Michaelis-Menten constants by pre-capillary reactions

A Michaelis-Menten analysis was firstly performed by a pre-capillary reaction format; Ty was used as a substrate with its concentrations ranging between 0.02−0.2 mmol L^{-1}. The kinetic analysis was performed at three reaction time of 5, 10, or 15 min to investigate the effect of product accumulation on K_m. A typical electropherogram by the pre-capillary reaction is shown in Fig. 3. Reaction products of Do and Dc are detected in addition to the substrate Ty. It is known that Dq is instantly cyclized and converted to Dc, and therefore, Dq was not detected. It has been reported that Ty has three pK_a values of 2.30, 9.28 and 10.28, Do has four pK_a values of 2.31, 8.71, 9.74 and 13.4, and Dc has three pK_a values of 0.8, 3.1 and 9.1 [7]. Considering the pH condition of the separation buffer (pH = 9.2), the net anionic charge is in the order of Ty < Do < Dc. The migration order agrees with the anionic charge; less anionic Ty migrates at the first and most anionic Dc is the last. Peak areas of Do and Dc increased with the reaction time from 5 min to 15 min.

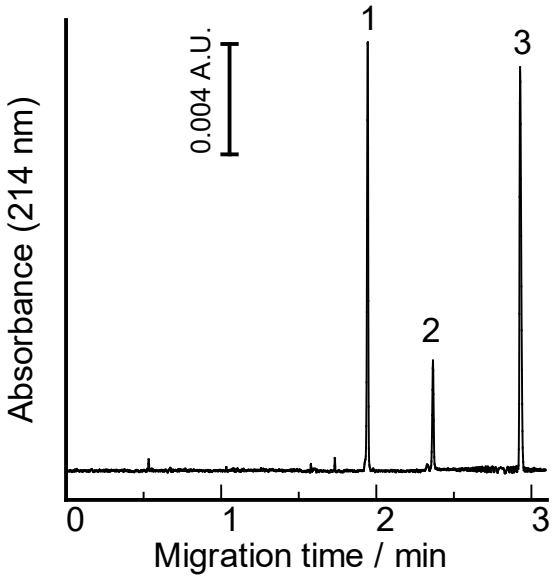

Fig. 3. A typical electropherogram for L-tyrosine by a pre-capillary reaction. The reaction solution contained 0.1 mmol L^{-1} tyrosine, 0.02 mg mL^{-1} TRS, and 10 mmol L^{-1} phosphate buffer (pH 7.0). The solution was incubated at 30 °C for 10 min in a vial. The separation buffer contained 10 mmol L^{-1} borax (pH 9.2). CE conditions: 50 mbar × 3 s sample injection, 25 kV applied voltage, 214 nm detection wavelength, and 30 °C capillary temperature. Peak identifications: 1, L-tyrosine; 2, L-dopa; 3, dopachrome.

Michaelis-Menten curves using the peak area of Do or Dc are shown in Fig. 4. The results were analyzed with Eq. (1), and $K_{m,Ty}$ value was determined by a nonlinear least-squares analysis. Results are summarized in Table 1. It can be noted that the $K_{m,Ty}$ value increased with increasing reaction time. The results suggest that the product inhibition would be serious with accumulated products. Values of $K_{m,Ty}$ reported by CE analyses are 0.05334 mmol L^{-1} [21] (analyzed by the amount of Do produced), 0.374 mmol L^{-1} [25] and 0.636 mmol L^{-1} [26] (analyzed by substrate reduction without product identification). The values are widely distributed, and results in this study are comparable with the reported data. The wide distribution of the $K_{m,Ty}$ value would be attributed to the less consideration on the influence of the amount of products, as well as the product inhibition.

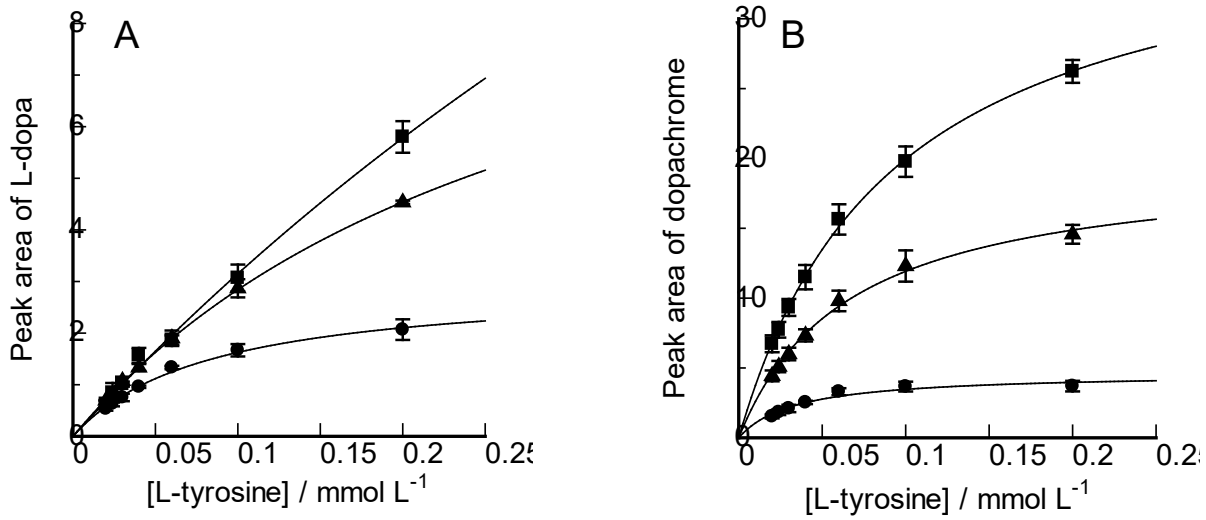

Fig. 4. Michaelis-Menten curves for L-tyrosine. A, peak area of L-dopa was used for the analysis; B, peak area of dopachrome was used for the analysis. Incubation time: ●, 5 min; ▲, 10 min; ■ 15 min.

Table 1 $K_{m,Ty}$ value determined by a pre-capillary reaction in this study.

Reaction time	$K_{m,Ty}$ / mmol L^{-1} *	
	From Do	From Dc
5 min	0.083 ± 0.008	0.034 ± 0.006
10 min	0.30 ± 0.02	0.066 ± 0.005
15 min	1.01 ± 0.4	0.092 ± 0.004

* Uncertainty: standard error.

A Michaelis-Menten analysis was also performed with an enzymatic reaction from Do to Dc. Figure 5A shows a typical electropherogram obtained by the enzymatic oxidation of Do; two peaks attributed to the substrate Do and the product Dc are detected. Michaelis-Menten curves are shown in Fig. 5B, where peak area of Dc has been used as the reaction rate. Michaelis-Menten constant of $K_{m,Do}$ is summarized in Table 2. Result obtained in this study is also comparable to the reported values of 0.502 mmol L^{-1} [23], 1.347 mmol L^{-1} [24] and 1.78 mmol L^{-1} [22]. The $K_{m,Do}$ value did not scatter so much with the reaction time, compared with $K_{m,Ty}$. This result indicates that the effect of product inhibition on the enzymatic reaction is rather little.

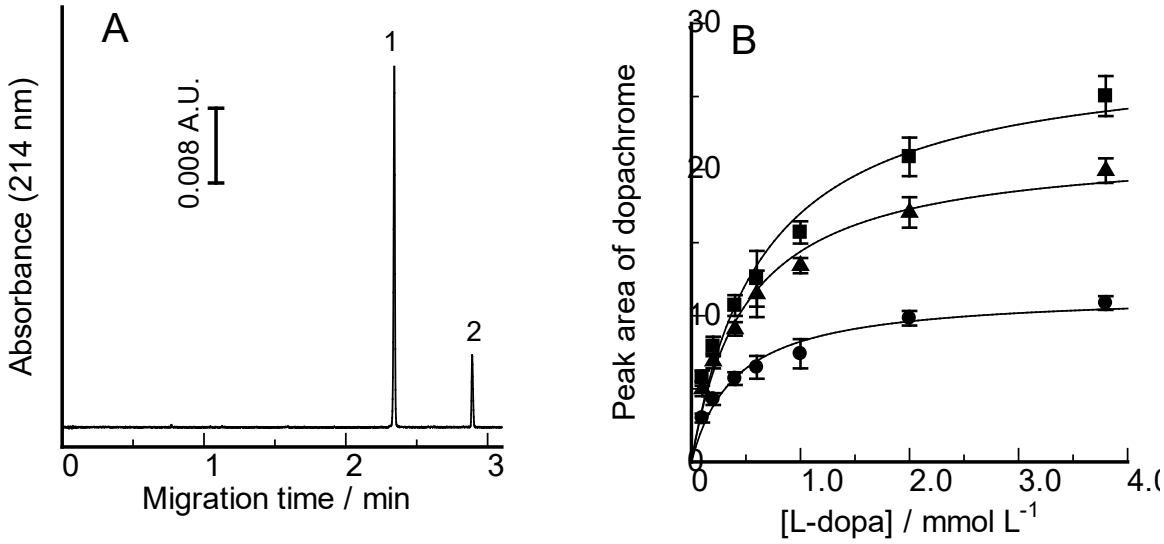

Fig. 5. A typical electropherogram for L-dopa (A) and Michaelis-Menten curves (B) by a pre-capillary reaction. The reaction solution contained 0.1 mmol L^{-1} dopa, 0.004 mg mL^{-1} TRS, and 10 mmol L^{-1} phosphate buffer (pH 7.0). Reaction conditions, the separation buffer, and CE conditions are the same as in Fig. 3. Peak identifications: 1, L-dopa; 2, dopachrome. Incubation time: ●, 5 min; ▲, 10 min; ■ 15 min.

Table 2 $K_{m,Do}$ value determined by pre-capillary reaction in this study.

Reaction time	$K_{m,Do}$ / mmol L^{-1} *
5 min	0.40 ± 0.08
10 min	0.50 ± 0.08
15 min	0.65 ± 0.10

* Uncertainty: standard error.

4.2 Determination of a Michaelis-Menten constant of $K_{m,Do}$ by CE/DFA

Enzymatic oxidation from Do to Dq is a single-step reaction, and the second-step reaction was firstly examined by CE/DFA. When a CE/DFA is performed using Do as a substrate in a sample solution, a plateau signal of Dc would continuously be detected immediately after the detection of the substrate Do peak, as is illustrated in Fig. 2B(d). Figure 6 shows electropherograms of continuously detected Dc as a result of the enzymatic oxidation of Do; plateau signals of Dc are detected. As drawn in Fig. 1, this reaction is relatively fast, and the plateau signal tended to descend from the start of the enzymatic reaction (late migration time) to the detection just after the enzymatic reaction (migration time adjacent to the substrate Do). The descending is attributed to the consumption of the substrate and gradual decrease in the substrate concentration. An increase was also observed at the start of the enzymatic reaction. A short induction period would be necessary for the

stable reaction rate of the enzymatic reaction. Therefore, highest point of the plateau signal was used for the Michaelis-Menten analysis. The height of the plateau signal increased with the increase in the substrate concentration. A Michaelis-Menten curve is drawn in Fig. 6B, where the height of the plateau signal of Dc was directly used as a reaction rate.-A Michaelis-Menten constant of $K_{m,Do}$ = 0.45±0.03 mmol L^{-1} was obtained by a nonlinear least-squares analysis. The value is close to the $K_{m,Do}$ value determined by the pre-capillary reaction in this study.

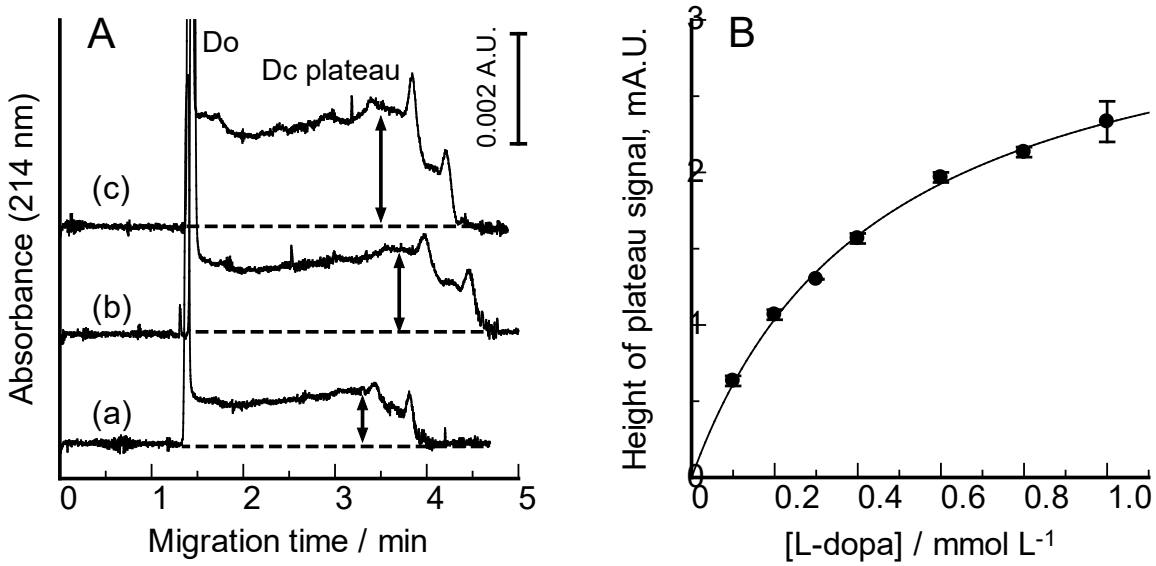

Fig. 6. Typical electropherograms for L-dopa under CE/DFA (A) and a Michaelis-Menten curve (B). Concentrations of L-dopa in the sample solution: (a) 0.2 mmol L^{-1}, (b) 0.4 mmol L^{-1}, (c) 0.6 mmol L^{-1}. The separation buffer contained 10 mmol L^{-1} phosphate buffer (pH 7.0) and 0.02 mg mL^{-1} TRS. CE conditions: 50 mbar × 3 s sample injection, 20 kV applied voltage, 214 nm detection wavelength, and 30 ºC capillary temperature.

4.3 Determination of a Michaelis-Menten constant of $K_{m,Ty}$ by CE/DFA

When the first-step enzymatic reaction from Ty to Do with TRS is subjected, the formation rate of Do is to be measured by CE/DFA. However, both Ty and Do are electrically neutral at pH 7.0 suitable for the enzymatic reaction, and they are not resolved by the electrophoresis. Fortunately, Do is an intermediate species in the enzymatic oxidation, and it is further converted to anionic Dq and Dc. The finally formed Dc is then separated from the substrate zone. It is also helpful that the reaction rate from Do to Dq is sufficiently faster than that from Ty to Do; the formed Do would immediately be converted to Dc. Therefore, enzymatically formed Do would be quantified as a plateau signal of Dc.

A calibration graph of Do was prepared for this aim. The concentration of an enzyme TRS was set at 4 times higher than the in-capillary reaction from Do to Dc, because the reaction rate from Ty to Do is much slower. Additionally, the concentration of Do produced from Ty would not be so high, and the calibration graph of Do was examined at 10^{-5} mol L^{-1} level. The concentration of Do was not sufficiently high in the CE/DFA and Do was rapidly consumed and the plateau signal descended to the baseline level in the electropherograms (Fig. 7A). However, a narrow plateau was successfully detected at the start of the electrophoresis/enzymatic reaction. A calibration graph is drawn with the highest points of the plateau; the result is shown in Fig. 7B. The calibration graph is linear against Do concentration at 10^{-5} mol L^{-1} level. The plateau height of Dc produced from Ty would be quantified with this calibration curve to estimate the amount of the intermediate Do produced from Ty.

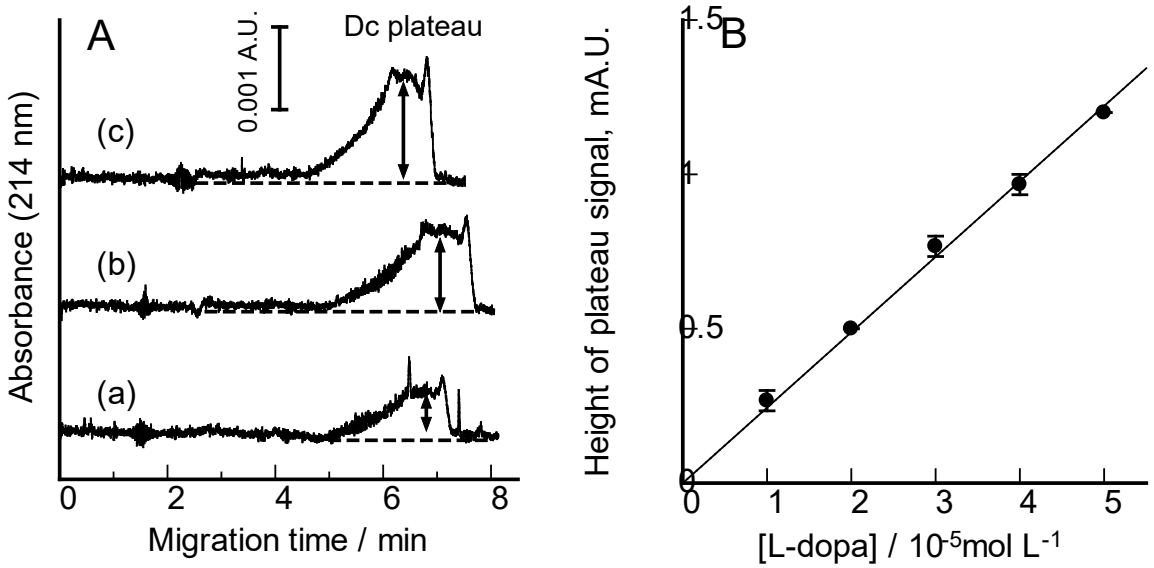

Fig. 7. Electropherograms for the calibration curve of L-dopa in CE/DFA (A), and a calibration curve for L-dopa (B). Concentrations of L-dopa in the sample solution: (a) 0.02 mmol L^{-1}, (b) 0.04 mmol L^{-1}, (c) 0.05 mmol L^{-1}. The separation buffer contained 10 mmol L^{-1} phosphate buffer (pH 7.0) and 0.08 mg mL^{-1} TRS. CE conditions: 50 mbar × 3 s sample injection, 12 kV applied voltage, 214 nm detection wavelength, and 30 °C capillary temperature.

Figure 8A shows electropherograms of the plateau signal of Dc, when Ty was used as a substrate. The conditions are the same as in Fig. 7; the preparation of the calibration graph for Do. It is helpful for CE/DFA that the degree of the reaction rates is $k_{Ty} < k_{Do}$, since the generation of Do from Ty is the rate-

determining step and the steadily formed Do is immediately converted to Dc. Detection of a plateau signal of Dc suggests that the intermediate Do was continuously generated from Ty at a steady rate. The height of the plateau signal of Dc increased with increasing concentrations of a substrate Ty. The height of the plateau signal was reduced to a steadily generated concentration of Do with the calibration graph of Fig. 7B. A Michaelis-Menten curve for Ty by the CE/DFA is shown in Fig. 8B. A Michaelis-Menten constant, $K_{m,Ty}$, was determined through a nonlinear least-squares analysis and a value of 0.061 ± 0.009 mmol L^{-1} was obtained. The $K_{m,Ty}$, value obtained by the CE/DFA is close to the result with a short reaction time in the pre-capillary reaction. Therefore, it can be said that product inhibition was favorably avoided in CE/DFA and that more reliable K_m value would be determined without the product inhibition. In this way, CE/DFA can analyze the reactions from Ty to Do and from Do to Dq, independently.

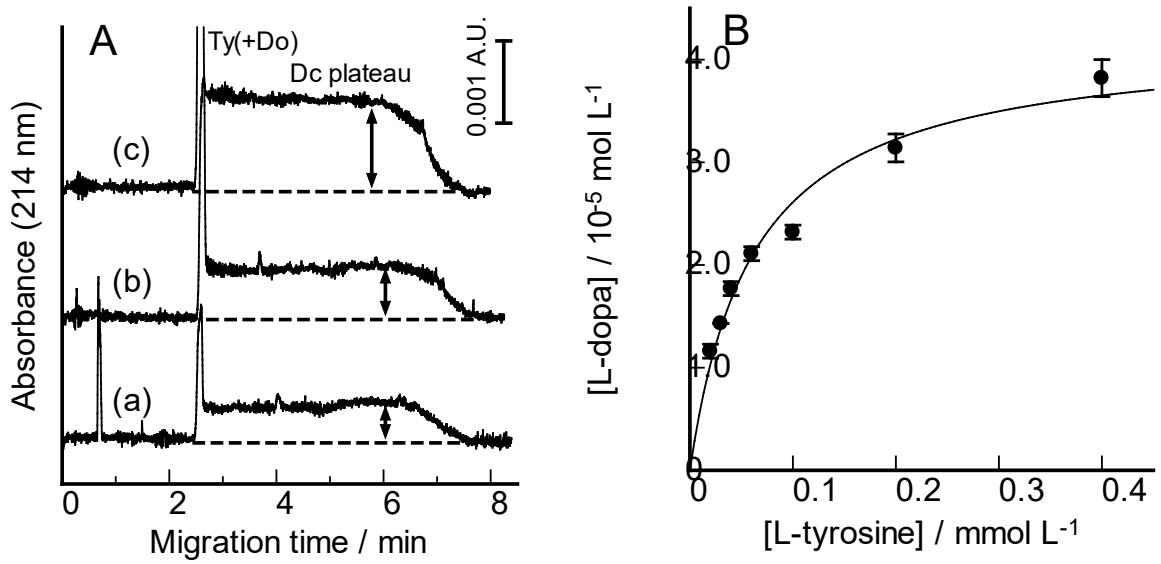

Fig. 8. Typical electropherograms for L-tyrosine under CE/DFA (A) and a Michaelis-Menten curve (B). Concentrations of L-tyrosine in the sample solution: (a) 0.06 mmol L^{-1}, (b) 0.1 mmol L^{-1}, (c) 0.2 mmol L^{-1}. The separation buffer and CE conditions are the same as in Fig. 7.

4.4 Comparison of the product inhibition in Michaelis-Menten constants

It can be noted with Michaelis-Menten constants that the values determined by the proposed CE/DFA are smaller than the ones determined by the pre-capillary reaction. Additionally, the difference is greater with the first-step enzymatic reaction from Ty to Do. The K_m is practically defined as the dissociation constant of the enzyme-substrate complex (ES) to form an enzyme (E) and a substrate (S) as in an equilibrium constant

(2).

$$K_m = \frac{[E][S]}{[ES]} \quad (2)$$

A larger K_m value suggests that the complex ES is more dissociable, and the complex is not likely to be formed. The reaction product is continuously removed from the reaction field of the substrate zone by CE/DFA, and thus the formation of the ES complex is promoted. In other words, product inhibition is suppressed or excluded at the substrate zone by CE/DFA. In conventional analytical methods, product inhibitions have traditionally been avoided and corrected by measuring the initial reaction rate before the product increases. However, the treatment is such analysis as under a quasi-steady state [33]. On the other hand, CE/DFA includes the removal of the product, and the enzymatic reaction kinetics are ideally done under a steady state, even if reversible reactions may accompany. As a result, the K_m value would be determined without product inhibition. The difference in K_m values between the proposed CE/DFA and a traditional analysis suggests the degree of the product inhibition, *vice versa*. Because the $K_{m,Ty}$ value is larger in the pre-capillary reaction format, more seriously with longer incubation time, the product inhibition is unavoidable in the pre-capillary format or traditional batch analyses. In contrast, an almost identical $K_{m,Do}$ value was obtained by pre-capillary reaction with different reaction time (Table 2). The result suggests that the product inhibition is little. It is also supported by the fact that the $K_{m,Do}$ value determined by CE/DFA is close to the value determined by the pre-capillary reaction. Therefore, it would be convenient to know the degree of the product inhibition by comparing the K_m values obtained by the pre-capillary reaction and by CE/DFA.

5. Conclusions

In this study, two-steps enzymatic oxidation of tyrosine with TRS were analyzed through a conventional pre-capillary reaction and a proposed CE/DFA. The two-steps reactions, from Ty to Do and from Do to Dq, were independently analyzed by the two analysis methods. A plateau signal of Dc was commonly detected as a plateau signal in CE/DFA on both substrates of Ty and Do. Two Michaelis-Menten constants of $K_{m,Ty}$ and $K_{m,Do}$ were successfully determined through the plateau signal. Advantage on using CE/DFA is the exclusion of the product inhibition by the electrophoretic resolution of the product from the substrate zone.

Obtained $K_{m,Do}$ value was comparable between the pre-capillary reaction and the CE/DFA, suggesting that the product inhibition is little. On the other hand, $K_{m,Ty}$ value determined by the pre-capillary reaction got larger with the reaction time, and it was also larger than the one determined by the CE/DFA. These results suggested that the product inhibition is serious in the first-step enzymatic reaction. Usefulness of the CE/DFA was demonstrated in two-steps enzymatic reactions with this TRS study.

Funding: This work was supported by a Grant-in-Aid for Scientific Research (C) (No. 20K05568) from the Japan Society for the Promotion of Sciences (JSPS).

Conflicts of interest/Competing interests: The authors declare that they have no conflict of interest.

References

1. R. Saruno, F. Kato, T. Ikeno, Kojic acid, a tyrosinase inhibitor from *Aspergillus albus*, Agric. Biol. Chem. 43 (1979) 1337−1338. https://doi.org/10.1271/bbb1961.43.1337.
2. J. N. Rodríguez-López, L.G. Fenoll, M.J. Peñalver, P.A. García-Ruiz, R. Varón, F. Martínez-Ortíz, F. García-Cánovas, J. Tudela, Tyrosinase action on monophenols: evidence for direct enzymatic release of *o*-diphenol, Biochim. Biophys. Acta 1548 (2001) 238−256. https://doi.org/10.1016/S0167-4838(01)00237-0.
3. Z.-Z. Pan, H.-L. Li, X.-J. Yu, Q.-X. Zuo, G.-X. Zheng, Y. Shi, X. Liu, Y.-M. Lin, G. Liang, Q. Wang, Q.-X. Chen, Synthesis and antityrosinase activities of alkyl 3,4-dihydroxybenzoates, J. Agric. Food Chem. 59 (2011) 6645−6649. https://doi.org/10.1021/jf200990g.
4. W.M. Chai, R. Wang, M.K. Wei, Z.R. Zou, R.G. Deng, W.S. Liu, Y.Y. Peng, Proanthocyanidins extracted from *Rhododendron pulchrum* leaves as source of tyrosinase inhibitors: structure, activity, and mechanism, PLOS ONE 10 (2015) e0145483. https://doi.org/10.1371/journal.pone.0145483.
5. M.R. Loizzo, R. Tundis, F. Menichini, Natural and synthetic tyrosinase inhibitors as antibrowning agents: an update, Compr. Rev. Food Sci. Food Saf. 11 (2012) 378−398. https://doi.org/10.1111/j.1541-4337.2012.00191.x.
6. Y.-J. Kim, H. Uyama, Tyrosinase inhibitors from natural and synthetic sources: structure, inhibition mechanism and perspective for the future, Cell. Mol. Life Sci. 62 (2005) 1707−1723.

https://doi.org/10.1007/s00018-005-5054-y.

7. G.M. Robinson, M.R. Smyth, Simultaneous determination of products and intermediates of L-dopa oxidation using capillary electrophoresis with diode-array detection, Analyst 122 (1997) 797−802. https://doi.org/10.1039/A701844D.

8. S. Fayad, P. Morin, R. Nehmé, Use of chromatographic and electrophoretic tools for assaying elastase, collagenase, hyaluronidase, and tyrosinase activity, J. Chromatogr. A 1529 (2017) 1−28. https://doi.org/10.1016/j.chroma.2017.11.003.

9. H. Zhang, M. Lu, H. Jiang, Z.-Y. Wu, D.-D. Zhou, D.-Q. Li, F.-Q. Yang, Tyrosinase-mediated dopamine polymerization modified magnetic alginate beads for dual-enzymes encapsulation: Preparation, performance and application, Colloid Surf. B 188 (2020) 110800. https://doi.org/10.1016/j.colsurfb.2020.110800.

10. J.J. Bao, J.M. Fujima, N.D. Danielson, Determination of minute enzymatic activities by means of capillary electrophoretic techniques, J. Chromatogr. B 699 (1997) 481−497. https://doi.org/10.1016/S0378-4347(96)00244-7.

11. Y. Fan, G.K.E. Scriba, Advances in-capillary electrophoretic enzyme assays, J. Pharm. Biomed. Anal. 53 (2010) 1076−1090. https://doi.org/10.1016/j.jpba.2010.04.005.

12. J. Bao, F.E. Regnier, Ultramicro enzyme assays in a capillary electrophoretic system, J. Chromatogr. A 608 (1992) 217−224. https://doi.org/10.1016/0021-9673(92)87127-T.

13. B.J. Harmon, D.H. Patterson, F.E. Regnier, Electrophoretically mediated microanalysis of ethanol, J. Chromatogr. A 657 (1993) 429−434. https://doi.org/10.1016/0021-9673(93)80298-M.

14. D.H. Patterson, B.J. Harmon, F.E. Regnier, Electrophoretically mediated microanalysis of calcium, J. Chromatogr. A 662 (1994) 389−395. https://doi.org/10.1016/0021-9673(94)80526-1.

15. H. Nehme, R. Nehme, P. Lafite, S. Routier, P. Morin, New development in in-capillary electrophoresis techniques for kinetic and inhibition study of enzymes, Anal. Chim. Acta 722 (2012) 127−135. https://doi.org/10.1016/j.aca.2012.02.003.

16. J. Iqbal, An enzyme immobilized microassay in capillary electrophoresis for characterization and inhibition studies of alkaline phosphatases, Anal. Biochem. 414 (2011) 226−231. https://doi.org/10.1016/j.ab.2011.03.021.

17. J. Iqbal, S. Iqbal, C.E. Müller, Advances in immobilized enzyme microbioreactors in capillary

electrophoresis, Analyst 138 (2013) 3104−3116. https://doi.org/10.1039/C3AN00031A.

18. Q.-Q. Li, F.-Q. Yang, Y.-Z. Wang, Z.-Y. Wu, Z.-N. Xia, H. Chen, Evaluation of thrombin inhibitory activity of catechins by online capillary electrophoresis-based immobilized enzyme microreactor and molecular docking, Talanta 185 (2018) 16−22. https://doi.org/10.1016/j.talanta.2018.03.049.
19. S.M. Krylova, V. Okhonin, S.N. Krylov, Transverse diffusion of laminar flow profiles - a generic method for mixing reactants in capillary microreactor, J. Sep. Sci. 32 (2009) 742−756. https://doi.org/10.1002/jssc.200800671.
20. E. Farcaş, L. Pochet, M. Fillet, Transverse diffusion of laminar flow profiles as a generic capillary electrophoresis method for in-line nanoreactor mixing: Application to the investigation of antithrombotic activity, Talanta 188 (2018) 516−521. https://doi.org/10.1016/j.talanta.2018.06.014.
21. T.-F. Jiang, T.-T. Liang, Y.-H. Wang, W.-H. Zhang, Z.-H. Lv, Immobilized capillary tyrosinase microreactor for inhibitor screening in natural extracts by capillary electrophoresis, J. Pharm. Biomed. Anal. 84 (2013) 36−40. https://doi.org/10.1016/j.jpba.2013.05.023.
22. M. Cheng, Z. Chen, Screening of tyrosinase inhibitors by capillary electrophoresis with immobilized enzyme microreactor and molecular docking, Electrophoresis 38 (2017) 486−493. https://doi.org/10.1002/elps.201600367.
23. L. Tang, W. Zhang, H. Zhao, Z. Chen, Tyrosinase inhibitor screening in traditional Chinese medicines by electrophoretically mediated microanalysis, J. Sep. Sci. 38 (2015) 2887−2892. https://doi.org/10.1002/jssc.201500371.
24. D.-M. Liu, J.-L. Yang, W. Ha, J. Chen, Y.-P. Shi, Kinetics and inhibition study of tyrosinase by pressure mediated microanalysis, Anal. Biochem. 525 (2017) 54−59. https://doi.org/10.1016/j.ab.2017.02.020.
25. B.-B. Sun, L. Qi, X.-Y. Mu, J, Qiao, M.-L. Wang, A chiral ligand exchange CE system for monitoring inhibitory effect of kojic acid on tyrosinase, Talanta 116 (2013) 1121−1125. https://doi.org/10.1016/j.talanta.2013.08.028.
26. Y. Su, X. Mu, L. Qi, A new chiral ligand exchange capillary electrophoresis system based on Zn(II)-L-leucine complexes coordinating with β-cyclodextrin and its application in screening tyrosinase inhibitors, RSC Adv. 4 (2014) 55280−55285. https://doi.org/10.1039/C4RA09433F.
27. T. Takayanagi, M. Mine, H. Mizuguchi, Capillary electrophoresis/dynamic frontal analysis for the enzyme assay of 4-nitrophenyl phosphate with alkaline phosphatase, Anal. Sci. 36 (2020) 829−834.

https://doi.org/10.2116/analsci.19P471.

28. M. Mine, H. Mizuguchi, T. Takayanagi, Inhibition assay of theophylline by capillary electrophoresis/dynamic frontal analysis on the hydrolysis of *p*-nitrophenyl phosphate with alkaline phosphatase, Chem. Lett. 49 (2020) 681−684. https://doi.org/10.1246/cl.200130.
29. M. Mine, N. Matsumoto, H. Mizuguchi, T. Takayanagi, Kinetic analysis of an enzymatic hydrolysis of *p*-nitrophenyl acetate with carboxylesterase by pressure-assisted capillary electrophoresis/dynamic frontal analysis, Anal. Methods 12 (2020) 5846−5851. https://doi.org/10.1039/D0AY01736A.
30. M. Mine, H. Mizuguchi, T. Takayanagi, Kinetic analysis of substrate competition in enzymatic reactions with β-D-galactosidase by capillary electrophoresis / dynamic frontal analysis, J. Pharm. Biomed. Anal. 188 (2020) 113390. https://doi.org/10.1016/j.jpba.2020.113390.
31. M. Mine, H. Mizuguchi, T. Takayanagi, Kinetic analysis of the transphosphorylation with creatine kinase by pressure-assisted capillary electrophoresis/dynamic frontal analysis, Anal. Bioanal. Chem. 413 (2021) 1453−1460. https://doi.org/10.1007/s00216-020-03110-9.
32. The R Project for Statistical Computing. https://www.r-project.org/ (accessed 9 April 2022).
33. S. Schäuble, A.K. Stavrum, P. Puntervoll, S. Schuster, I. Heiland, FEBS Lett. 587 (2013) 2818−2824. https://doi.org/10.1016/j.febslet.2013.06.025.